中国光学（中英文） Chinese Optics 核心期刊

紫外偏振敏感的$CsPbBr_3$纳米薄膜的可见光发射

吉于今 楚学影 董旭 李金华

Visible light emission of ultraviolet polarization sensitive $CsPbBr_3$ nano-films

JI Yu-jin, CHU Xue-ying, DONG Xu, LI Jin-hua

引用本文:
吉于今, 楚学影, 董旭, 李金华. 紫外偏振敏感的$CsPbBr_3$纳米薄膜的可见光发射[J]. 中国光学, 2023, 16(1): 202-213. doi: 10.37188/CO.2022-0152
JI Yu-jin, CHU Xue-ying, DONG Xu, LI Jin-hua. Visible light emission of ultraviolet polarization sensitive $CsPbBr_3$ nano-films[J]. *Chinese Optics*, 2023, 16(1): 202-213. doi: 10.37188/CO.2022-0152

在线阅读 View online: https://doi.org/10.37188/CO.2022-0152

文章编号 2097-1842(2023)01-0202-12

Visible light emission of ultraviolet polarization sensitive $CsPbBr_3$ nano-films

JI Yu-jin[1,2], CHU Xue-ying[1,2*], DONG Xu[1], LI Jin-hua[1,2]
(1. *College of Physics*, *Changchun University of Science and Technology*, *Changchun* 130022, *China*;
2. *Nanophotonics and Biophotonics Key Laboratory of Jilin Province*, *Changchun* 130022, *China*)
* *Corresponding author*, *E-mail*: *xueying_chu@cust.edu.cn*

Abstract: In order to detect polarized ultraviolet light by visible optical elements, $CsPbBr_3$ nanocrystal/metal wire-grid composited films were prepared. The stability of its fluorescence was improved by depositing Al_2O_3 passivation layer. The green fluorescence of polarization-sensitive perovskite nanocrystals film was obtained under ultraviolet exciting light. The results show that the crystal structure of the $CsPbBr_3$ nanocrystals obtained by hot-injection method have a cubic crystal system structure with a square shape and an average size of about 39 nm. An obvious green fluorescence at about 530 nm were observed under ultraviolet light excitation of the nanocrystal colloidal solution. The fluorescence intensity of the $CsPbBr_3$ nanocrystal/metal wire-grid composited film obtained by self-assembly changed periodically with the polarization direction of the excited light. The luminous polarization ratio is about 0.54. The fluorescence intensity of this composite film was enhanced when Al_2O_3 was deposited on its surface by atomic layer deposition technology. The polarization ratio of the passivated film can still reach 0.36. The above results show that the fluorescence stability and polarization of perovskite nanocrystals film can be optimized by the surface passivation and the introduction of metal wire-grids, respectively. The obtained ultraviolet polarization sensitive $CsPbBr_3$ nanocrystals composited film exhibits important application value in the fields of ultraviolet polarization detection and liquid crystal display.

Key words: $CsPbBr_3$ nanocrystals; surface passivation; fluorescence enhancement; polarization

紫外偏振敏感的 $CsPbBr_3$ 纳米薄膜的可见光发射

吉于今[1,2], 楚学影[1,2*], 董 旭[1], 李金华[1,2]
(1. 长春理工大学 物理学院, 吉林 长春 130022;
2. 纳米光子学与生物光子学吉林省重点实验室, 吉林 长春 130022)

摘要: 为了利用可见光学元件实现对紫外偏振光的高性能探测, 制备了 $CsPbBr_3$ 纳米晶/金属线栅复合薄膜, 并通过向其

收稿日期: 2022-07-05; **修订日期:** 2022-07-25
基金项目: 吉林省科技厅科技发展计划项目(No. 20200201266JC)
Department of Science and Technology of Jilin Province (No. 20200201266JC)

表面沉积 Al_2O_3 钝化层提高了薄膜荧光稳定性，获得了紫外激发下偏振敏感的钙钛矿纳米晶薄膜绿色荧光。测试结果表明，以高温热注入法获得的 $CsPbBr_3$ 纳米晶为立方晶系结构，形貌呈方形，尺寸约 39 nm。以紫外光激发纳米晶胶体溶液可在 530 nm 处观测到明显的绿色荧光。以自组装方法获得的 $CsPbBr_3$ 纳米晶/金属线栅复合薄膜荧光发光强度随紫外激发光的偏振方向呈周期性变化，其发光偏振度约为 0.54。以原子层沉积技术向此复合薄膜表面沉积 Al_2O_3 层可明显提高其荧光强度，钝化后复合薄膜的发光偏振度仍可达 0.36。以上结果表明，表面钝化和引入金属线栅方法可分别优化钙钛矿纳米晶薄膜的荧光稳定性和荧光偏振度，所获得的紫外偏振敏感的 $CsPbBr_3$ 纳米晶复合薄膜在紫外偏振探测以及液晶显示等领域具有重要的应用价值。

关　键　词: $CsPbBr_3$ 纳米晶；表面钝化；荧光增强；偏振
中图分类号: O469　　**文献标志码:** A　　**doi:** 10.37188/CO.2022-0152

1 Introduction

In recent years, all-inorganic perovskite $CsPbX_3$ (X=Cl, Br, I) nanocrystals (NCs) have attracted extensive attention due to their excellent optoelectronic properties[1-2], such as high fluorescence quantum yield, narrow half-peak width, adjustable bandgap, high absorption coefficient and high carrier mobility[3], and have broad application prospects in the fields of light-emitting diodes[4], liquid crystal displays[5], photodetectors[6-7] and lasers[8].

At present, the preparation methods of all-inorganic perovskite NCs mainly include hot-injection method, ligand-assisted reprecipitation method, room temperature synthesis method, etc. Among them, the hot-injection method is favored by people because the NCs with regular morphology and relatively small size distribution can be obtained by this method. However, studies have found that due to the ionic properties of perovskite NCs[9], perovskite NCs prepared by various methods have fluorescence instability[10-11] to a certain extent when they are exposed to humidity and light, and are made into devices, which is the primary problem restricting its industrialization. In recent years, important progress has been made in improving the fluorescence stability of all-inorganic perovskite quantum dots by introducing ligands during hot-injection method. However, for perovskite quantum dot films, which are easier to be applied in practice, the related research is very rare. The environment and the state of the ligand may both have changed after film formation, so related research is particularly important. Refs. [12-14] show that deposition of metal oxides (ZnO, Al_2O_3, etc.) on the surface of NCs with atomic layer deposition technology[12] can effectively improve their stability, and encapsulation of NCs can improve the stability of NC films and their luminous properties[15-16]. However, the perovskite quantum dot films need to be further researched.

The polarized luminescent properties of perovskite NCs are another concern besides stability. Since the Protesescu research group synthesized inorganic halide perovskite ($CsPbX_3$, X=Cl, Br, I) NCs in 2015, Sun *et al*. have studied the fluorescence polarization characteristics of $CsPbX_3$ NCs, and their measurement results show that the polarization degree of $CsPbBr_3$ is 0.08[17]; Zhong *et al*. embedded perovskite NCs in polymer composite films, and the degree of polarization can be increased to 0.3 through the controllable mechanical stretching. However, after long-term illumination, the fluorescence luminous intensity has a large degree of attenuation[18]. Therefore, the construction of perovskite quantum dot films with both high fluorescence stability and high polarization characteristics is still an important issue worth exploring.

Metal wire-grid[19] with a micro-nano scale structure and good polarization performance is widely used in the field of polarization devices such as optical communication and liquid crystal display. In this paper, it is proposed that the $CsPbBr_3$ NCs modified by Al_2O_3 can be compounded with metal wire-grids to achieve high stability and high polariz-

ation luminescence films. With the assistance of the hot-injection method, $CsPbBr_3$ NCs colloidal solution was synthesized by the ligand modification of the sample with high fluorescence stability reported in the literature. $CsPbBr_3$ NCs/metal wire-grid composite films were obtained by self-assembly method, and Al_2O_3 passivation layer was deposited on the surface of the composite films by atomic layer deposition technology. The effect of Al_2O_3 passivation layer on the fluorescence intensity of the composite film was compared and analyzed, and the effect of Al_2O_3 deposition on the polarization characteristics of $CsPbBr_3$ NCs/metal wire-grid composite film was studied.

2 Experiment

2.1 Experimental materials

Cesium carbonate (Cs_2CO_3, 99.99%), Lead bromide ($PbBr_2$, 99.99%), Oleic acid (OA, AR), 1-Octadecene (ODE, 90%), and (3-Aminopropyl) triethoxysilane (APTES, 97%) were purchased from Aladdin Reagent Company, ethyl acetate was purchased from Tianjin Fuyu Fine Chemical Co., Ltd., n-hexane was purchased from Beijing Chemical Plant, metal wire-grid was purchased from Jiangyin Yunxiang Photonics Co., Ltd.

2.2 Preparation of $CsPbBr_3$ NCs

Preparation of cesium oleate precursor: weigh 0.407 g (1.25 mmol) Cs_2CO_3, put it into a 50 mL four-necked bottle containing 20 mL ODE and 1.2 mL OA, heat the mixed solution in an N_2 environment with a magnetic stirring heater to 120 °C and keep it for 30 minutes, and then continue to raise the temperature to 150 °C to fully react the reactants until the solution is clear and transparent, then keep the obtained precursor at 100 °C for use.

Synthesis of $CsPbBr_3$ NCs: weigh 0.069 g $PbBr_2$, put it into a 50 mL three-necked bottle containing 5 mL ODE, 0.5 mL OA and 0.5 mL APTES, heat the mixed solution to 120 °C with a magnetic stirring heater in the N_2 environment for 30 minutes, then continue to raise the temperature to 170 °C, quickly inject 0.4 mL of cesium oleate precursor, react for 1 min, and quickly cool it to room temperature in an ice-water bath. After final cleaning and purification, dissolve in n-hexane for storage.

2.3 Preparation of composite films

Configure a certain concentration of $CsPbBr_3$ NC solution, use the metal wire-grid as the substrate, and lift the mechanical arm of the Langmuir-Blodgett system through the vertical lifting method, so that the $CsPbBr_3$ NCs and the metal wire-grid are recombined, and finally $CsPbBr_3$ NCs/ metal wire-grid composite film is obtained.

The Al_2O_3 passivation layer was deposited on the surface of the composite film by atomic layer deposition technology. The process is as follows: with trimethylaluminate as aluminum source and deionized water as oxygen source, the processes of each deposition cycle include water pulse (t_1), N_2 purge (t_2), aluminate pulse (t_3) and N_2 Purge (t_4), the pulse durations are: t_1=0.02 s; t_2=5 s; t_3=0.02 s; t_4=5 s.

2.4 Sample testing and characterization

The microscopic morphology of NCs particles was characterized by Transmission Electron Microscope (TEM, TecnaiG220S Twin) and Scanning Electron Microscope (SEM, JSM-6010LA), the structural characteristics of the samples are characterized by X-ray diffraction (XRD, D/MAX-Ultima), the absorption spectrum was measured by a UV-Vis spectrophotometer (SHIMADZU, UV-2450), and the fluorescence spectrum was measured by a fluorometer (SHIMADZU, RF-5301pc). In order to investigate the effect of light irradiation on the luminescence properties of $CsPbBr_3$ NCs/metal wire-grid composite films with or without Al_2O_3 film passivation, a 325nm He-Cd laser was used to irradiate the sample surface for 60 min, respectively, and Raman (Luminescence) spectrometer (labRAM HR E) was used to characterize the photoluminescence characteristics of the sample, and the laser power density on the surface of the sample was 3.15 $mW \cdot cm^{-2}$. All tests were done at RT.

3　Results and discussion

3.1　Phase and morphology analysis of $CsPbBr_3$ NCs

The $CsPbBr_3$ NCs colloidal solution was drop-coated on a silicon wafer to form a thin film, and the results of testing its XRD pattern are shown in Fig. 1 (color online). It can be seen from the Fig. 1. that all the diffraction peaks correspond to the JCPDS standard card (PDF#18-0364), and that the prepared $CsPbBr_3$ NCs are cubic crystal system. The samples have main diffraction peaks at 2θ of 15.21°, 21.69°, 30.74°, 37.73°, and 43.90°, corresponding to the crystallographic planes (100), (110), (200), (211), and (202) of $CsPbBr_3$ crystals, respectively, which shows that the crystal has good crystallinity.

Fig. 2(a) shows the results of characterizing the morphology of the obtained $CsPbBr_3$ NCs by TEM. It can be found that the NCs have a square shape. As shown in Fig. 2(b), the statistics of all particle size distributions. show that the average size of NCs is about 39 nm. Fig. 2(c) shows the SEM image of the $CsPbBr_3$ NCs film. It can be seen from the Fig. 2(c). that the size of the obtained NCs is relatively uniform and in the shape of a cube, which is basically consistent with the results of TEM. Fig. 2(d) is the SEM image of the $CsPbBr_3$ NCs film after Al_2O_3 passivation, and it can be found that the Al_2O_3 passivation did not significantly change the surface morphology of the nanofilm.

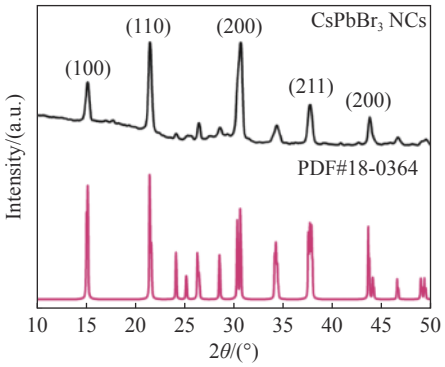

Fig. 1　XRD spectrum (top) of $CsPbBr_3$ NCs film and standard diffraction pattern (bottom) of $CsPbBr_3$

图 1　$CsPbBr_3$ 纳米晶薄膜的 XRD 图谱和 $CsPbBr_3$ 的标准衍射图谱

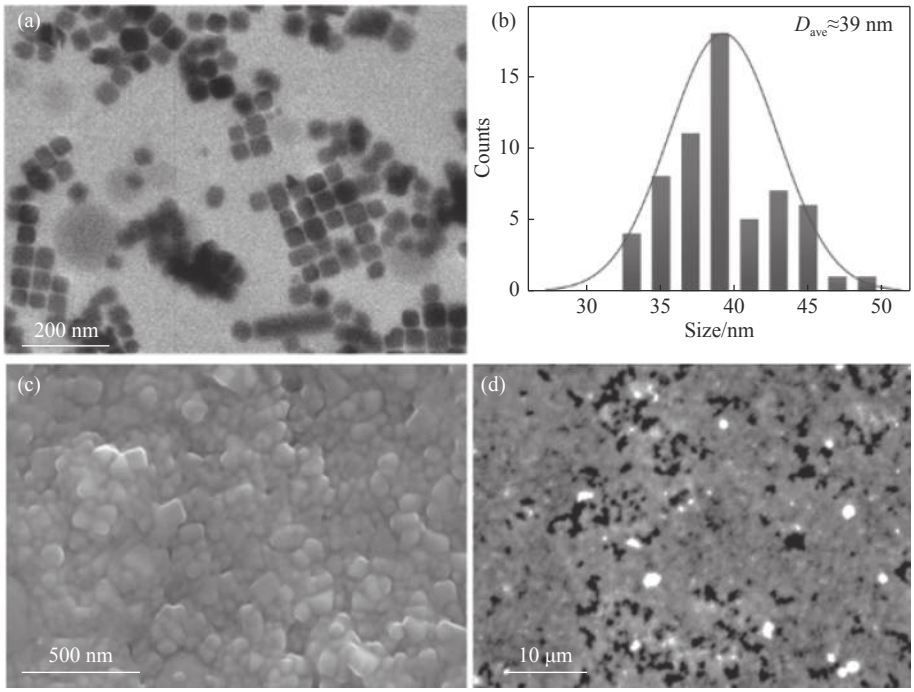

Fig. 2　(a) TEM images of $CsPbBr_3$ NCs; (b) the size distribution of the NCs; (c) SEM images of $CsPbBr_3$ NCs; (d) $CsPbBr_3$ NCs films after Al_2O_3 passivation

图 2　(a)$CsPbBr_3$ 纳米晶 TEM 图像; (b) 纳米晶尺寸分布; (c)$CsPbBr_3$ 纳米晶薄膜 SEM 图像; (d)Al_2O_3 钝化后 $CsPbBr_3$ 纳米晶薄膜 SEM 图像

The absorbance of the $CsPbBr_3$ NCs solution was measured by a UV-Vis spectrometer, as shown by the dotted line in Fig. 3(a) (color online), which has an obvious absorption peak at 510 nm and a band gap of 2.34 eV. The solid line in Fig. 3(a) is the fluorescence emission spectrum of $CsPbBr_3$ NCs excited by 365 nm ultraviolet light, the luminescent center is located near 530 nm, and its half-maximum width is only 16.18 nm, indicating that the obtained $CsPbBr_3$ NCs have excellent luminescent properties. Fig. 3(b) (color online) and Fig. 3(c) (color online) are the physical sample photographs of $CsPbBr_3$ NCs sol under visible light and the ultraviolet lamp, from which it can be found that the NCs colloid solution of synthesis is yellow-green and an intense green fluorescence is observed under UV lamp irradiation.

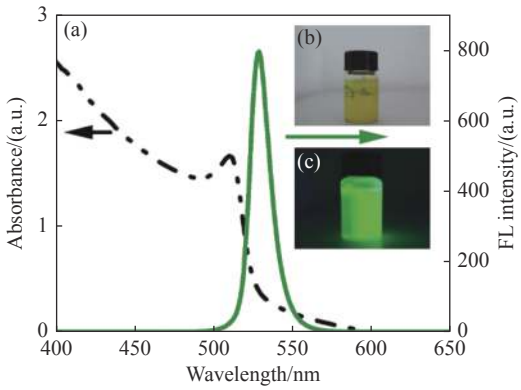

Fig. 3 (a) UV-Vis absorption spectrum (dotted line) and fluorescence (FL) emission spectrum (solid line) of the $CsPbBr_3$ NCs; optical photographs of $CsPbBr_3$ NCs under (b) natural light and (c) UV light

图 3 (a) $CsPbBr_3$ 纳米晶的荧光光谱 (实线) 与紫外-可见吸收光谱图 (虚线); $CsPbBr_3$ 纳米晶在 (b) 自然光和 (c) 紫外光下的实物照片

3.2 Fluorescent properties and optimization of $CsPbBr_3$ NCs/metal wire-grid composite thin films

In order to take advantage of the excellent optical properties of $CsPbBr_3$ NCs to realize ultraviolet polarization optical detection, $CsPbBr_3$ NCs/metal wire-grid composite films were prepared by self-assembly on the metal wire-grid substrate. The solid line in Fig. 4(a) (color online) is the fluorescence emission spectrum of the composite film. It can be found that under the excitation of 325 nm laser, the composite film shows a sharp luminescence peak near 521 nm. Because the surface state has a great influence on the optical properties of perovskite quantum dots, a certain amount of Al_2O_3 is deposited on the surface of the $CsPbBr_3$/wire-grid composite film by atomic layer deposition method to optimize the optical properties of the composite film. The dotted line in Fig. 4(a) is the fluorescence emission spectrum of the composite film after Al_2O_3

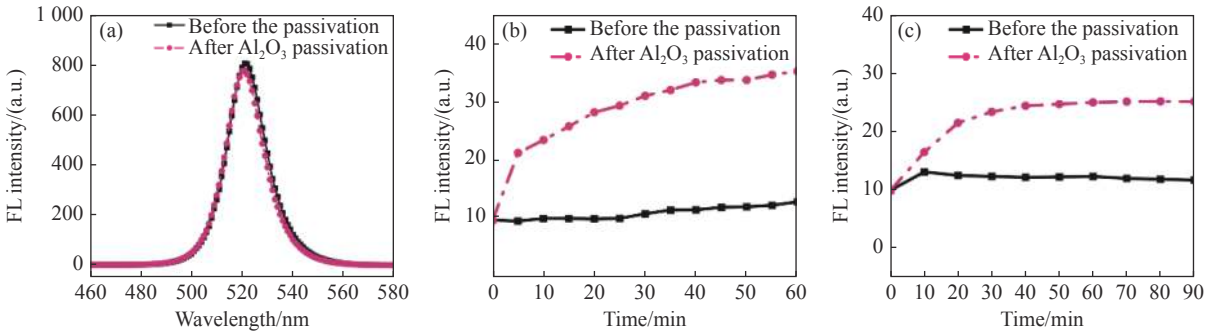

Fig. 4 (a) FL spectra of nanocrystal/metal wire-grid composite films before and after Al_2O_3 passivation; (b) plots of FL intensity of the $CsPbBr_3$ NCs/metal wire-grid composited film versus time of irradiation by UV light before and after Al_2O_3 passivation; (c) plots of FL intensity of the $CsPbBr_3$ NCs film versus time of irradiation by UV light before and after Al_2O_3 passivation (Dotted lines are for samples after Al_2O_3 passivation, and solid lines are for samples before the Al_2O_3 passivation)

图 4 (a) Al_2O_3 钝化前后纳米晶/金属线栅复合薄膜的荧光光谱图; (b) Al_2O_3 钝化前后 $CsPbBr_3$ 纳米晶/金属线栅复合薄膜荧光强度随紫外光照时间变化关系曲线; (c) Al_2O_3 钝化前后 $CsPbBr_3$ 纳米晶薄膜荧光强度随紫外光照时间变化关系曲线(每个图中虚线对应样品经 Al_2O_3 钝化后的结果; 实线对应样品未沉积 Al_2O_3 的结果)

deposition. The comparative analysis reveals that the fluorescence peak intensity of the thin film after coating with Al_2O_3 decreases to 96.47% of the original value, and the luminescence peak position has a red shift of about 1 nm and is accompanied by an increase in the half-peak width, which is due to the fact that the heating of the substrate platform during the atomic layer deposition experiment causes some of the NCs surface ligands to fall off, and the NCs are more likely to produce agglomeration at high temperatures, which enhances the electronic coupling of NCs[20].

Continuous laser irradiation studies show that the obtained composite films have good fluorescence stability. As shown by the solid line in Fig. 4(b), the fluorescence intensity of the $CsPbBr_3$ NCs/metal wire-grid composite film remains basically stable within 60 min of continuous irradiation with 325 nm laser (optical power density about 3.15 mW cm^{-2}). After Al_2O_3 passivation, the luminous intensity of the composite film can be continuously improved by increasing the irradiation time, and it can be enhanced to about 3.3 times of the initial value at 60 min. As a wide bandgap oxide, Al_2O_3 restricts the migration of photogenerated carriers in perovskite NCs films. Due to the suppression of high energy band gap, the photogenerated carriers and holes are confined inside $CsPbBr_3$ NCs[21], so that the luminous intensity of the composite thin film is enhanced after the Al_2O_3 is deposited on the thin film.

In order to verify the changing law of the influence of Al_2O_3 passivation on the fluorescence intensity of $CsPbBr_3$ NCs thin films, the fluorescence stability of $CsPbBr_3$ NCs thin films without metal wire-grids was further compared and analyzed. As shown in Fig. 4(c), within 90 min of continuous ultraviolet light irradiation, the fluorescence intensity of the $CsPbBr_3$ NCs film that has not been passivated by Al_2O_3 has a certain increase in the first 10 min, and then gradually decays to about 1.1 times of the initial fluorescence intensity; while the fluorescence intensity of the $CsPbBr_3$ NCs film passivated by Al_2O_3 increases with the increase of the irradiation time, and gradually stabilizes at about 2.5 times of the initial fluorescence intensity after about 40 min.

3.3　Polarization properties of $CsPbBr_3$ NCs/metal wire-grid composite films

The optical path shown in Fig. 5(a) is used to test the fluorescence polarization characteristics of the obtained $CsPbBr_3$ NCs/metal wire-grid composite thin film sample. With the linearly polarized ultraviolet light radiated by a He-Cd laser with a wavelength of 325 nm as the excitation light and the periodical adjustment on the polarization direction of the incident linearly polarized light by a UV 1/2λ wave plate with a rotatable spindle, the fluorescence signal of the sample is collected by a monochromator after removing the impact of the excitation light through ultraviolet filter.

Fig. 5(b) shows the fluorescence spectra of the $CsPbBr_3$ NCs/metal wire-grid composite film without Al_2O_3 passivation treatment under the excitation of ultraviolet light in different polarization directions. In order to clarify the change Law of fluorescence intensity more clearly, Figs. 5(c) 5(d) show the relationship curve of the fluorescence intensity at 521 nm with the polarization direction of incident light for the composite film without Al_2O_3 passivation treatment (5(c)), and with Al_2O_3 passivation treatment (5(d)). It can be found that within a cycle, the fluorescence peak intensities of the $CsPbBr_3$ NCs/metal wire-grid composite film before and after Al_2O_3 passivation show a cosine-like periodic variation pattern with the change of the polarization angle of the incident light, indicating that the composite film is sensitive to the polarization direction of the incident light, by which can realize the detection of the polarization direction of the incident light. The polarization degree of fluorescence[22-23] can be determined by the following equation[24]:

$$P = \frac{I_{max} - I_{min}}{I_{max} + I_{min}} \quad ,$$

where I_{max} and I_{min} represent the maximum value

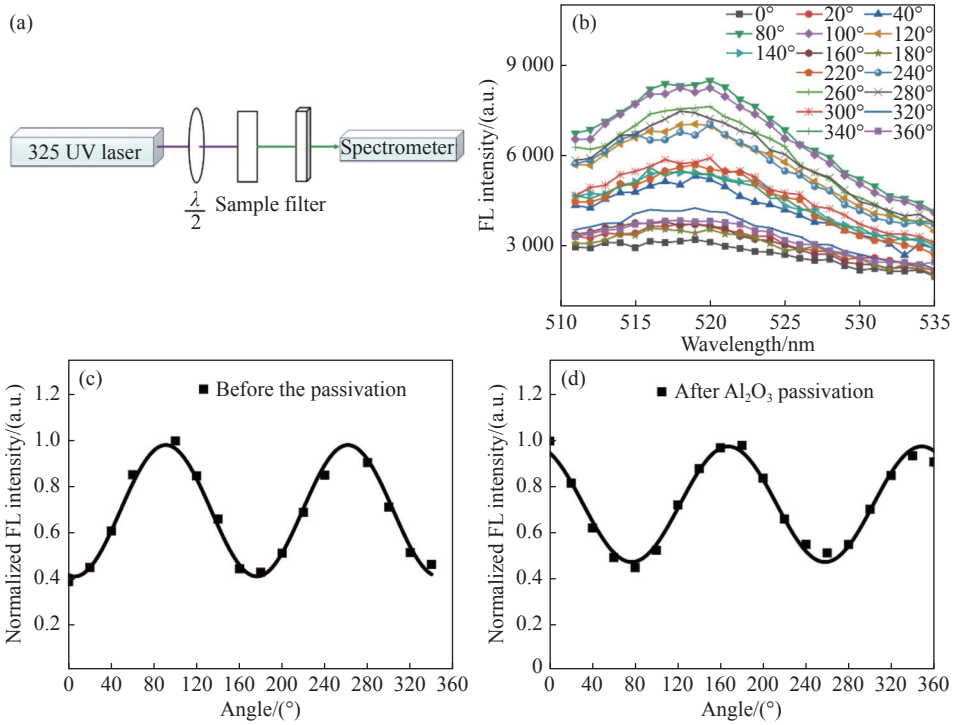

Fig. 5 (a) Schematic diagram of polarization fluorescence spectroscopy test; (b) FL spectra of $CsPbBr_3$ NCs/metal wire-grid composited films corresponding to different polarization angles of the exciting light; plots of FL intensities of the $CsPbBr_3$ NCs/metal wire-grid composited film before (c) and after (d) Al_2O_3 passivation versus the polarization angles of the exciting light

图 5 (a) 偏振荧光光谱测试原理图; (b) 不同激发光偏振角度对应的 $CsPbBr_3$ 纳米晶/金属线栅复合薄膜偏振荧光光谱图; Al_2O_3 钝化前后 $CsPbBr_3$ 纳米晶/金属线栅复合薄膜荧光强度随激发光角度变化曲线: (c) 钝化前, (d) 钝化后

and minimum value of the fluorescence luminous intensity of the composite thin film within a cycle of the incident light polarization angle change, respectively. It can be seen from the calculation that the fluorescence polarization of $CsPbBr_3$ NCs/metal wire-grid composite film is 0.54, while the fluorescence polarization of the composite film after Al_2O_3 surface passivation is 0.36, the above results are higher than the current existing results on the fluorescence polarization of $CsPbBr_3$ NCs films[17-18]. In summary, although Al_2O_3 passivation can enhance the fluorescence of composite films, the fluorescence polarization will be decreased after depositing isotropic Al_2O_3 on the surface of anisotropic composite films. The above results can provide reference experience for related follow-up research.

4 Conclusion

In this paper, cubic phase $CsPbBr_3$ NCs with good dispersion, uniform particle size distribution and average grain size of about 39 nm are successfully prepared by hot-injection method, and are used to obtain $CsPbBr_3$ NCs/metal wire-grid composite film by self-assembly technique, and then an Al_2O_3 passivation layer is deposited on the surface of the composite film by the atomic layer deposition technique. Fluorescent stability tests show that the photogenerated carrier confinement effect of the Al_2O_3 passivation layer significantly improves the luminous intensity and stability of the composite film under ultraviolet light. Polarization optical properties tests show that the fluorescence emission intensity of $CsPbBr_3$ NCs/metal wire-grid composite film is sensitive to the polarization direction of ultraviolet excitation light, and its fluorescence emission intensity changes periodically with the polarization angle of excitation light. The fluorescence polarization of the composite film without Al_2O_3 deposition is 0.54, and the polarization degree reduces to 0.36

after Al_2O_3 deposition. In summary, the deposition of Al_2O_3 passivation layer on the surface of $CsPbBr_3$ NCs/metal wire-grid composite film by atomic layer deposition technology can improve the stability and fluorescence intensity of the composite film, and the good polarization optical properties that exhibited by the composite film before and after passivation provide a way to prepare ultra-stable perovskite NCs semiconductor device materials with good performance, which have important research significance for the polarization detection of the conversion from ultraviolet to visible light.

——中文对照版——

1　引　言

近年来，全无机钙钛矿 $CsPbX_3$ (X=Cl, Br, I) 纳米晶因其优异的光电性能，包括高的荧光量子产率、窄的半峰宽、可调节的带隙、高的吸收系数以及高载流子迁移速率等[1-3] 而受到广泛关注，在发光二极管[4]、液晶显示[5]、光探测器[6-7] 以及激光器[8] 等领域具有广泛的应用前景。

目前，全无机钙钛矿纳米晶的制备方法主要有高温热注入法、配体辅助再沉淀法、室温合成法等，其中高温热注入法因所获得的纳米晶形貌规则，尺寸分布较窄，而受到人们青睐。但研究发现，由于钙钛矿纳米晶的离子特性[9]，导致在湿度、光照以及制作成器件时，各种方法制备的钙钛矿纳米晶均存在一定程度的荧光不稳定[10-11]，这是制约其产业化的首要难题。近年来，在提高全无机钙钛矿量子点荧光稳定性方面，人们通过在高温热注入过程中引入配体等手段取得了重要进展。但针对更易于实际应用的钙钛矿量子点薄膜，相关研究还非常少见。而成膜后量子点环境和配体状态可能均发生了改变，因此，相关研究显得尤为重要。文献调研表明，借助原子层沉积技术[12] 在纳米晶的表面沉积金属氧化物[13-14](ZnO, Al_2O_3 等) 可有效提高其稳定性，对纳米晶体进行包覆封装，从而提高纳米晶薄膜的稳定性，并对其发光特性进行改善[15-16]。但针对钙钛矿量子点薄膜的相关研究仍有待探讨。

钙钛矿纳米晶的偏振发光特性是除稳定性外，另一个值得关注的问题。自 Protesescu 课题组在 2015 年合成了无机卤化物钙钛矿（$CsPbX_3$, X=Cl, Br, I）纳米晶后，Sun 等人对 $CsPbX_3$ 纳米晶的荧光偏振特性进行了研究，测得 $CsPbBr_3$ 的偏振度为 0.08[17]；Zhong 等人将钙钛矿纳米晶嵌入聚合物复合薄膜，通过可控的机械拉伸方法，使偏振度提高到 0.3，但是经过长时间的光照后，荧光的发光强度有很大程度的衰减[18]。因此，构建同时具有高荧光稳定性和高偏振特性的钙钛矿量子点薄膜仍然是当前值得探索的重要问题。

金属线栅[19] 具有微纳米尺度结构，偏振性能好，广泛应用于光通讯及液晶显示等偏振器件领域。本文提出借助金属线栅与 Al_2O_3 修饰的 $CsPbBr_3$ 纳米晶复合，实现高稳定性和高偏振度发光的薄膜。采用文献报道中可获得高荧光稳定性样品的配体修饰辅助高温热注入法合成了 $CsPbBr_3$ 纳米晶胶体溶液。通过自组装方法获得 $CsPbBr_3$ 纳米晶/金属线栅复合薄膜，并以原子层沉积技术在复合薄膜表面沉积了 Al_2O_3 钝化层。对照分析了 Al_2O_3 钝化层对复合薄膜的荧光强度的影响，并针对沉积 Al_2O_3 对 $CsPbBr_3$ 纳米晶/金属线栅复合薄膜偏振特性的影响进行了研究。

2　实　验

2.1　实验材料

碳酸铯 (Cs_2CO_3, 99.99%)、溴化铅 ($PbBr_2$, 99.99%)、油酸 (Oleic acid, OA, AR)、十八烯 (1-Octadecene, ODE, 90%)、(3-氨丙基) 三乙氧基硅烷 ((3-Aminopropyl) triethoxysilane, APTES, 97%) 均购自阿拉丁试剂公司，乙酸乙酯购自天津市富宇精细化工有限公司，正己烷购自北京化工厂，金属线栅购自江阴韵翔光电技术有限公司。

2.2　$CsPbBr_3$ 纳米晶的制备

油酸铯前驱体的制备：称取 0.407 g(1.25 mmol) Cs_2CO_3，将其放入含 20 mL ODE 和 1.2 mL OA 的 50 mL 四颈瓶中，混合溶液在 N_2 环境中用磁力搅拌加热仪加热到 120 °C，并保持 30 分钟，然后继

续升高温度到 150 °C, 使反应物充分反应至溶液澄清透明后, 将得到的前驱体保持在 100 °C 待用。

$CsPbBr_3$ 纳米晶的合成: 称取 0.069 g $PbBr_2$, 将其放入含有 5 mL ODE、0.5 mL OA 和 0.5 mL APTES 的 50 mL 三颈瓶中, 混合溶液在 N_2 环境中用磁力搅拌均匀, 再将加热仪加热到 120 °C, 持续 30 分钟, 然后继续升高温度到 170 °C, 迅速注入油酸铯前驱体 0.4 mL, 反应 1 min 后快速冰水浴冷却至室温即可, 最终清洗提纯后溶于正己烷中保存。

2.3 复合薄膜的制备

配置一定浓度的 $CsPbBr_3$ 纳米晶溶液, 以金属线栅为衬底, 通过垂直提拉法提拉 Langmuir-Blodgett 拉膜机的机械臂, 使得 $CsPbBr_3$ 纳米晶与金属线栅复合, 最终获得 $CsPbBr_3$ 纳米晶/金属线栅复合薄膜。

使用原子层沉积技术在复合薄膜表面沉积 Al_2O_3 钝化层。过程如下: 以三甲基铝酸盐作为铝源, 去离子水作为氧源, 每个沉积周期包括水脉冲 (t_1)、N_2 吹扫 (t_2)、铝酸盐脉冲 (t_3) 和 N_2 吹扫 (t_4), 脉冲持续时间分别为: t_1=0.02 s; t_2=5 s; t_3=0.02 s; t_4=5 s。

2.4 样品的测试与表征

使用透射电子显微镜 (Transmission Electron Microscope, TEM, TecnaiG220S Twin) 和扫描电子显微镜 (Scanning Electron Microscope, SEM, JSM-6010LA) 表征纳米晶颗粒的微观形貌, 使用 X 射线衍射 (X-Ray Diffraction, XRD, D/MAX-Ultima) 表征样品的结构特征, 采用紫外-可见分光光度计 (SHIMADZU, UV-2450) 测定吸收光谱, 采用荧光分度计 (SHIMADZU, RF-5301pc) 测定荧光光谱。为了研究光辐照对有无 Al_2O_3 薄膜钝化的 $CsPbBr_3$ 纳米晶/金属线栅复合薄膜发光性能的影响, 使用 325 nm 的 He-Cd 激光器分别对样品表面进行 60 min 照射, 采用拉曼 (发光) 光谱仪 (labRAM HR E) 对样品进行光致发光特性的表征, 样品表面的激光功率密度为 3.15 $mW\cdot cm^{-2}$。所有测试均在室温下完成。

3 结果与讨论

3.1 $CsPbBr_3$ 纳米晶晶相和形貌分析

将 $CsPbBr_3$ 纳米晶胶体溶液滴涂在硅片上形成薄膜, 测试其 XRD 图谱, 结果如图 1(彩图见期刊电子版) 所示。从图中可知, 所有衍射峰与 JCPDS 标准卡 (PDF#18-0364) 相对应, 可知制备的 $CsPbBr_3$ 纳米晶为立方晶系。样品在 2θ 分别为 15.21°、21.69°、30.74°、37.73°、43.90°处出现主要衍射峰, 与 $CsPbBr_3$ 晶体的 (100)、(110)、(200)、(211)、(202) 晶面相对应, 说明晶体具有良好的结晶性。

利用 TEM 对所获得的 $CsPbBr_3$ 纳米晶体形貌进行表征, 结果如图 2(a) 所示。可以发现, 纳米晶呈方形形貌。对图中所有粒子尺寸分布进行统计, 可知纳米晶的平均尺寸约为 39 nm, 如图 2(b) 所示。图 2(c) 给出了 $CsPbBr_3$ 纳米晶薄膜的 SEM 图像。从图中可以看出, 所获得的纳米晶尺寸较为均匀, 呈立方体形状, 与 TEM 的结果基本一致。图 2(d) 为 Al_2O_3 钝化后 $CsPbBr_3$ 纳米晶薄膜的 SEM 图像, 可以发现 Al_2O_3 钝化未明显改变纳米薄膜的表面形貌。

通过紫外-可见光分度计测定 $CsPbBr_3$ 纳米晶溶液的吸光度, 如图 3(a)(彩图见期刊电子版) 中虚线所示, 其在 510 nm 处存在明显的吸收峰, 带隙为 2.34 eV。图 3(a) 中实线为 $CsPbBr_3$ 纳米晶在 365 nm 紫外光激发下的荧光发射光谱, 发光中心位于 530 nm 附近, 且其半高宽度仅为 16.18 nm, 表明所获得的 $CsPbBr_3$ 纳米晶具有优异的发光性能。图 3(b) (彩图见期刊电子版) 和图 3(c) (彩图见期刊电子版) 是 $CsPbBr_3$ 纳米晶溶胶在可见光与紫外光下的实物样品照片, 从照片中可以看出, 合成的纳米晶胶体溶液呈黄绿色, 且在紫外灯照射下可观察到强烈的绿色荧光。

3.2 $CsPbBr_3$ 纳米晶/金属线栅复合薄膜的荧光特性及优化

为了利用 $CsPbBr_3$ 纳米晶的优异光学特性实现紫外偏振光学探测, 以金属线栅为基底通过自组装方式制备了 $CsPbBr_3$ 纳米晶/金属线栅复合薄膜。图 4(a) (彩图见期刊电子版) 中实线为该复合薄膜的荧光发射光谱图。可以发现, 在 325 nm 激光的激发下, 复合薄膜在 521 nm 附近显示出尖锐的发光峰。这是因为表面态对钙钛矿量子点的光学性质有较大的影响, 采用原子层沉积方法向 $CsPbBr_3$/金属线栅复合薄膜表面沉积一定量的 Al_2O_3, 对复合薄膜的光学性质进行优化。图 4(a) 中虚线为沉积 Al_2O_3 之后复合薄膜的荧光发射光谱图。对照分析可发现, 包覆 Al_2O_3 后薄膜荧光

峰值强度降为原来的 96.47%, 发光峰位有 1 nm 左右的红移且伴随半峰宽的增加, 这是因为原子层沉积实验过程中, 基底平台加热会使部分纳米晶表面配体脱落, 高温时纳米晶更容易产生团聚现象, 使得纳米晶的电子耦合增强[20]。

连续激光辐照研究结果表明, 所获得的复合薄膜具有良好的荧光稳定性。如图 4(b) 中实线所示, $CsPbBr_3$ 纳米晶/金属线栅复合薄膜在 325 nm 激光(光功率密度约 3.15 mW·cm^{-2})连续辐照 60 min 内, 荧光强度基本保持稳定。而经 Al_2O_3 钝化后, 增加辐照时间可使得复合薄膜的发光强度不断提高, 60 min 时其可增强为初始值的 3.3 倍左右。Al_2O_3 作为宽禁带氧化物, 限制了钙钛矿纳米晶薄膜中的光生载流子迁移, 由于高能带隙的抑制作用, 光生载流子和空穴被限制在 $CsPbBr_3$ 纳米晶内部[21], 使得复合薄膜的发光强度在沉积 Al_2O_3 薄膜后荧光强度有一定的增强。

为了验证 Al_2O_3 钝化对 $CsPbBr_3$ 纳米晶薄膜荧光强度的影响规律, 进一步对照分析了未复合金属线栅的 $CsPbBr_3$ 纳米晶薄膜的荧光稳定性。如图 4(c) 所示, 在紫外光连续照射 90 min 内, 未被 Al_2O_3 钝化的 $CsPbBr_3$ 纳米晶薄膜的荧光发光强度在前 10 min 内有一定的增强, 而后逐渐衰减至初始荧光强度的 1.1 倍左右; 而经 Al_2O_3 钝化后的 $CsPbBr_3$ 纳米晶薄膜的荧光强度则随着辐照时间的延长而增大, 约 40 min 后逐渐稳定在初始荧光光强的 2.5 倍左右。

3.3　$CsPbBr_3$ 纳米晶/金属线栅复合薄膜的偏振特性

采用如图 5(a) 所示的光路对所获得的 $CsPbBr_3$ 纳米晶/金属线栅复合薄膜样品进行荧光偏振特性测试。以波长为 325 nm 的 He-Cd 激光器辐射的线偏振紫外光为激发光, 以可旋转主轴的紫外 1/2λ 波片对入射线偏振光的偏振方向进行周期性调节, 紫外滤光片去除激发光影响后, 样品的荧光信号由单色仪采集。

图 5(b) 给出了未进行 Al_2O_3 钝化处理的 $CsPbBr_3$ 纳米晶/金属线栅复合薄膜在不同偏振方向紫外光激发下的荧光光谱图。为了更清晰地说明荧光强度的变化规律, 图 5(c) 给出了未进行 Al_2O_3 钝化处理复合薄膜 521 nm 处荧光强度随入射光偏振方向的变化关系曲线, 图 5(d) 给出了 Al_2O_3 钝化后复合薄膜在 521 nm 处荧光强度随入射光偏振方向的变化关系曲线。可以发现, 在一个周期内, Al_2O_3 钝化前后 $CsPbBr_3$ 纳米晶/金属光栅复合薄膜荧光峰强度均随入射光偏振角度的改变而呈类余弦的周期性变化规律, 说明复合薄膜对入射光的偏振方向敏感, 可实现对入射光偏振方向的检测。荧光偏振度[22-23] 可以由以下公式[24] 确定:

$$P = \frac{I_{\max} - I_{\min}}{I_{\max} + I_{\min}} \quad ,$$

其中, $I_{\max}$与$I_{\min}$分别表示入射光偏振角度在一个周期内变化时, 复合薄膜荧光发光强度的最大值与最小值。通过计算可知, $CsPbBr_3$ 纳米晶/金属线栅复合薄膜的荧光偏振度为 0.54, 而经 Al_2O_3 表面钝化后复合薄膜的荧光偏振度为 0.36, 以上结果均高于当前关于 $CsPbBr_3$ 纳米晶薄膜荧光偏振度的已有结果[17-18]。综上可知, 虽然 Al_2O_3 钝化可实现复合薄膜荧光增强, 但在各向异性的复合薄膜表面沉积各向同性的 Al_2O_3 后, 会导致其荧光偏振度降低。以上结果可为后续相关研究提供经验。

4　结　论

本文采用高温热注入法成功制备出分散性良好、粒径分布均匀、平均晶粒约 39 nm 的立方相 $CsPbBr_3$ 纳米晶, 利用自组装技术获得了 $CsPbBr_3$ 纳米晶/金属线栅复合薄膜, 并通过原子层沉积技术向复合薄膜表面沉积 Al_2O_3 钝化层。荧光稳定性测试结果表明, Al_2O_3 钝化层的光生载流子限制效应使得紫外光照下复合薄膜的发光强度和稳定性有明显提高。偏振光学特性测试表明, $CsPbBr_3$ 纳米晶/金属线栅复合薄膜的荧光发射强度对紫外激发光的偏振方向敏感, 其荧光发光强度随激发光偏振角度呈周期性变化。未沉积 Al_2O_3 的复合薄膜荧光偏振度为 0.54, 沉积 Al_2O_3 后, 各向同性钝化层的引入使得其偏振度降低为 0.36。综上所述, 通过原子层沉积技术在 $CsPbBr_3$ 纳米晶/金属线栅复合薄膜表面沉积 Al_2O_3 钝化层可提高复合薄膜的稳定性和荧光发光强度, 钝化前后, 复合薄膜均表现出良好的偏振光学特性。本文研究结果为制备性能良好的超稳定钙钛矿纳米晶半导体器件材料提供了一种思路, 对实现紫外光波段向可见光波段转化的偏振探测具有重要的研究意义。

References:

[1] PROTESESCU L, YAKUNIN S, BODNARCHUK M I, *et al*.. Nanocrystals of cesium lead halide perovskites ($CsPbX_3$, X = Cl, Br, and I): novel optoelectronic materials showing bright emission with wide color gamut[J]. *Nano Letters*, 2015, 15(6): 3692-3696.

[2] 曲家沂, 王云鹏, 孙俊杰, 等. 光损伤肖特基钙钛矿探测器的光电特性分析[J]. 中国光学, 2022, 15(4): 668-674.
QU J Y, WANG Y P, SUN J J, *et al*.. Analysis of photoelectric characteristics of a light-damaged schottky perovskite detector[J]. *Chinese Optics*, 2022, 15(4): 668-674. (in Chinese)

[3] ZHANG Y N, SIEGLER T D, THOMAS C J, *et al*.. A "tips and tricks" practical guide to the synthesis of metal halide perovskite nanocrystals[J]. *Chemistry of Materials*, 2020, 32(13): 5410-5423.

[4] CHIBA T, HOSHI K, PU Y J, *et al*.. High-efficiency perovskite quantum-dot light-emitting devices by effective washing process and interfacial energy level alignment[J]. *ACS Applied Materials & Interfaces*, 2017, 9(21): 18054-18060.

[5] WANG Y, LI X M, SONG J ZH, *et al*.. All-inorganic colloidal perovskite quantum dots: a new class of lasing materials with favorable characteristics[J]. *Advanced Materials*, 2015, 27(44): 7101-7108.

[6] SURENDRAN A, YU X CH, BEGUM R, *et al*.. All inorganic mixed halide perovskite nanocrystal-graphene hybrid photodetector: from ultrahigh gain to Photostability[J]. *ACS Applied Materials & Interfaces*, 2019, 11(30): 27064-27072.

[7] 朱晓秀, 葛咏, 李建军, 等. 量子点增强硅基探测成像器件的研究进展[J]. 中国光学, 2020, 13(1): 62-74.
ZHU X X, GE Y, LI J J, *et al*.. Research progress of quantum dot enhanced silicon-based photodetectors[J]. *Chinese Optics*, 2020, 13(1): 62-74. (in Chinese)

[8] 王兰, 董渊, 高嵩, 等. 钙钛矿材料在激光领域的研究进展[J]. 中国光学, 2019, 12(5): 993-1014.
WANG L, DONG Y, GAO S, *et al*.. Research progress of perovskite materials in the field of lasers[J]. *Chinese Optics*, 2019, 12(5): 993-1014. (in Chinese)

[9] WANG B, LIU L J, LIU B, *et al*.. Study on fluorescence properties and stability of Cu^{2+}-Substituted $CsPbBr_3$ perovskite quantum dots[J]. *Physica B*:*Condensed Matter*, 2020, 599: 412488.

[10] WEI Y, CHENG Z Y, LIN J. An overview on enhancing the stability of lead halide perovskite quantum dots and their applications in phosphor-converted LEDs[J]. *Chemical Society Reviews*, 2019, 48(1): 310-350.

[11] 孙智国, 吴晔, 魏昌庭, 等. Ni^{2+}掺杂和卤素空位填充协同抑制$CsPbBr_3$纳米晶体中的离子迁移[J]. 中国光学, 2021, 14(1): 77-86.
SUN ZH G, WU Y, WEI CH T, *et al*.. Suppressed ion migration in halide perovskite nanocrystals by simultaneous Ni^{2+} doping and halogen vacancy filling[J]. *Chinese Optics*, 2021, 14(1): 77-86. (in Chinese)

[12] LOIUDICE A, SARIS S, OVEISI E, *et al*.. $CsPbBr_3$ QD/AlO_x inorganic nanocomposites with exceptional stability in water, light, and heat[J]. *Angewandte Chemie International Edition*, 2017, 56(36): 10696-10701.

[13] YIN B, SADTLER B, BEREZIN M Y, *et al*.. Quantum dots protected from oxidative attack using alumina shells synthesized by atomic layer deposition[J]. *Chemical Communications*, 2016, 52(74): 11127-11130.

[14] JING Y, CAO K, ZHOU B Z, *et al*.. Two-step hybrid passivation strategy for ultrastable photoluminescence perovskite nanocrystals[J]. *Chemistry of Materials*, 2020, 32(24): 10653-10662.

[15] XIANG Q Y, ZHOU B Z, CAO K, *et al*.. Bottom up stabilization of $CsPbBr_3$ quantum dots-silica sphere with selective surface passivation via atomic layer deposition[J]. *Chemistry of Materials*, 2018, 30(23): 8486-8494.

[16] CHENG C Y, MAO M H. Photo-stability and time-resolved photoluminescence study of colloidal CdSe/ZnS quantum dots passivated in Al_2O_3 using atomic layer deposition[J]. *Journal of Applied Physics*, 2016, 120(8): 083103.

[17] WANG D, WU D, DONG D, *et al*.. Polarized emission from $CsPbX_3$ perovskite quantum dots[J]. *Nanoscale*, 2016, 8(22): 11565-11570.

[18] ZHOU Q CH, BAI Z L, LU W G, *et al*.. In situ fabrication of halide perovskite nanocrystal-embedded polymer composite films with enhanced photoluminescence for display backlights[J]. *Advanced Materials*, 2016, 28(41): 9163-9168.

[19] 姜建娟. 金属微纳结构对荧光的调控[D]. 南京: 南京大学, 2015.
JIANG J J. *The modulation of fluorescence via metallic microstructured materials*[D]. Nanjing: Nanjing University, 2015. (in Chinese)

[20] MOYEN E, KANWAT A, CHO S, *et al*.. Ligand removal and photo-activation of $CsPbBr_3$ quantum dots for enhanced optoelectronic devices[J]. *Nanoscale*, 2018, 10(18): 8591-8599.

[21] LI J H, ZHAO D X, MENG X Q, *et al*.. Enhanced ultraviolet emission from ZnS-coated ZnO nanowires fabricated by self-assembling method[J]. *The Journal of Physical Chemistry B*, 2006, 110(30): 14685-14687.

[22] GÜNER T, TOPÇU G, SAVACI U, *et al*.. Polarized emission from $CsPbBr_3$ nanowire embedded-electrospun PU fibers[J]. *Nanotechnology*, 2018, 29(13): 135202.

[23] 韩琦, 吕飞逸, 王虎, 等. 全无机钙钛矿$CsPbBr_3$微米棒偏振荧光特性的研究[J]. 半导体光电, 2019, 40(6): 810-814.
HAN Q, LV F Y, WANG H, *et al*.. Investigation on polarization fluorescence properties of all-inorganic perovskite $CsPbBr_3$ microrods[J]. *Semiconductor Optoelectronics*, 2019, 40(6): 810-814. (in Chinese)

[24] SHI ZH F, LI Y, LI S, *et al*.. Polarized emission effect realized in $CH_3NH_3PbI_3$ perovskite nanocrystals[J]. *Journal of Materials Chemistry C*, 2017, 5(34): 8699-8706.

Author Biographics:

Ji Yu-jin (1994—), female, born in Yuncheng, Shanxi Province. In 2018, she received her bachelor's degree from Taiyuan Normal University in 2018. Currently, she is mainly engaged in the research of nanomaterial preparation and optical properties. E-mail: yj_ji1113@163.com
吉于今 (1994—), 女, 山西运城人, 硕士研究生, 2018 年于太原师范学院获得学士学位, 主要从事纳米材料制备及光学特性方面的研究。E-mail: yj_ji1113@163.com

Chu Xue-ying (1982—), female, born in Changchun, Jilin Province, Ph.D., associate Professor. In 2011, she obtained her Ph.D. degree from Northeast Normal University. Currently, she is mainly engaged in the research on the preparation of semiconductor nanomaterials and the application of photoelectric properties. E-mail: xueying_chu@cust.edu.cn
楚学影 (1982—), 女, 吉林长春人, 博士, 副教授, 2011 年于东北师范大学获得博士学位, 主要从事半导体纳米材料制备及光电特性应用方面的研究。E-mail: xueying_chu@cust.edu.cn